

A simple tight-binding approach to topological superconductivity in monolayer MoS₂

H Simchi^{1,2,†}¹Department of Physics, Iran University of Science and Technology, Narmak, Tehran 16844, Iran²Iran Semiconductor Technology Center, Tehran 19575-199, Iran

(Received 10 October 2019; revised manuscript received 12 December 2019; accepted manuscript online 24 December 2019)

Monolayer molybdenum disulfide (MoS₂) has a honeycomb crystal structure. Here, with considering the triangular sublattice of molybdenum atoms, a simple tight-binding Hamiltonian is introduced (derived) for studying the phase transition and topological superconductivity in MoS₂ under uniaxial strain. It is shown that spin-singlet p + ip wave phase is a topological superconducting phase with nonzero Chern numbers. When the chemical potential is greater (smaller) than the spin-orbit coupling (SOC) strength, the Chern number is equal to four (two) and otherwise it is equal to zero. Also, the results show that, if the superconductivity energy gap is smaller than the SOC strength and the chemical potential is greater than the SOC strength, the zero energy Majorana states exist. Finally, we show that the topological superconducting phase is preserved under uniaxial strain.

Keywords: MoS₂, topological superconductivity, Chern number, band inversion**PACS:** 74.78.-w, 74.20.Rp, 74.25.Dw, 74.70.Xa**DOI:** 10.1088/1674-1056/ab6552

1. Introduction

A monolayer of molybdenum disulfide (MoS₂), which has a honeycomb crystal structure, is a prototypical transition-metal dichalcogenide (TMD). Its phonon-limited room temperature mobility is dominated by the optical deformation potential and polar optical scattering versus Frohlich interaction.^[1] The dominating deformation potentials originate from couplings to the intervalley longitudinal optic (LO) and homopolar phonons.^[1] It should be noted that due to the valley degeneracy in the conduction band, both intervalley and intravalley scatterings of carriers should be considered for calculating the electron-phonon coupling constant.^[1] Roldan *et al.* have studied the origin of superconductivity in heavily doped MoS₂ by considering the electron-phonon and electron-electron interactions.^[2] They have shown that the intravalley (intervalley) electron-phonon coupling constant is equal to -0.36 (-0.13).^[2] It has been shown that heavily gated thin films of MoS₂ become superconductive.^[3,4] The Rashba spin-orbit coupling (RSOC) arise in the experiment due to the presence of the strong gating field of the order of 10 MeV/cm.^[5-7] The RSOC induced two superconducting phases which can be topologically nontrivial.^[8] Lu *et al.* have shown that the Zeeman field, which is originated from the intrinsic SOC induced by breaking in-plane inversion symmetry, pins the spin orientation of the electrons to the out-of-plane direction and protects the Ising superconductivity in gated MoS₂.^[9] Also, it has been shown how the spin-triplet p-wave pairing symmetry affects the superconducting excitations.^[1]

From civil practical point of view, increasing the critical temperature of superconductors (T_c) is a necessary condition.

For increasing T_c , both the density of states (DOS) and the vibration frequency of a superconducting material should be high.^[11] For non-metallic materials or materials which have low DOS, applying strain and doping can be an effective method to induce superconductivity.^[12] The elastic bending modulus of monolayer MoS₂ has been studied and it has been shown that the binding modulus is equal to 9.61 eV.^[13] Woo *et al.* have used a first-principle approach and studied the elastic properties of layered two-dimensional materials.^[14] They have found that the Poisson's ratios of graphene, h-BN, and 2H-MoS₂ along the out-of-plane direction are negative, near zero, and positive, respectively, whereas their in-plane Poisson's ratios are all positive.^[14] Two important and main crystal deformations are mechanical deformation and curvature of crystal lattice. The bond lengths of TMDs are changed under mechanical deformations and in consequence their electronic structures are changed due to the corrections in the electronic Hamiltonian. However, the curvature of the crystal lattice mixes the orbital structure of the electronic Bloch bands. Pearce *et al.* have presented an effective low energy Hamiltonian for describing the effects of mechanical deformations and curvature on the electronic properties of monolayer TMDs.^[15] In sodium intercalated bilayer MoS₂, the electron-phonon interaction strength changes and the superconductivity is significantly enhanced due to the strain effect.^[16] Similar work has been reported about calcium doped MoS₂ bilayer recently.^[14] Finally, Kang *et al.* have reported the discovery of Holstein polarons (a small composite particle of an electron that carries a cloud of phonons) in a surface-doped layered semiconductor MoS₂^[18] and He *et al.* have shown that

†Corresponding author. E-mail: simchi@alumni.iust.ac.ir

in a wide range of experimentally accessible regime where the in-plane magnetic field is higher than the Pauli limit field but lower than second critical magnetic field, a 2H-structure monolayer NbSe₂ or similarly TaS₂ becomes a nodal topological superconductor.^[19]

In this paper, we study the spin-singlet p + ip topological superconductivity in monolayer MoS₂ using a simple tight-binding Hamiltonian when the crystal is (not) under uniaxial strain.

Xiao *et al.* have considered the molecular orbitals d_{z^2} and $1/\sqrt{2}(d_{x^2-y^2} + i\tau d_{xy})$ as basis functions of conduction and valence bands, respectively ($\tau = \pm 1$ is the valley index). They have shown that, to the first order in k , the C_{3h} symmetry dictates a two-band $\mathbf{k} \cdot \mathbf{p}$ Hamiltonian.^[2] Cappelluti *et al.* have shown that the $4d_{3z^2-r^2}$ (82%), $3p_x, 3p_y$ (12%), and other orbitals (6%) contribute in constructing the minimum of the conduction band (MCB).^[21] Roldan *et al.* have studied the superconductivity effect in heavily doped MoS₂ by considering the $d_{3z^2-r^2}$ orbital as the main orbital component.^[2] The possible topological superconductivity phase^[8] and strongly enhanced superconductivity^[12] in MoS₂ have been studied. In both studies, the $d_{3z^2-r^2}$ orbital is considered as the main orbital component.^[8,12] Therefore, we consider a single band Hamiltonian model including the intrinsic SOC (ISOC) and RSOC near K and K' points and show that there are two band inversion (nodal) points which separate unoccupied states from occupied ones in the phase diagram. Using the threefold rotation symmetry of the crystal and the properties of rotation fixed points Γ , K , and K' , we calculate the Chern number.^[22] It is shown that when the chemical energy is greater (smaller) than the ISOC strength, the Chern number is equal to four (two) and otherwise it is equal to zero. Since, the $4d_{z^2}$ orbital is the dominant component of the states we only consider the Mo-layer with triangular lattice structure for doing the numerical calculations. The Mo-layer has both flat and zigzag edges but we consider a zigzag nanoribbon of Mo-layer and introduce a simple tight-binding Hamiltonian for studying the topological superconductivity in MoS₂. It is shown that when the superconductivity energy gap is smaller than the ISOC and the chemical potential is greater than the ISOC, the zero energy Majorana states exist. Finally, we show that the topological superconducting phase is preserved under uniaxial strain. Using a simple tight binding method and crystal symmetry for studying the topological properties and justifying the effect of uniaxial strain on the topological properties are the novelties of the article in comparison with the other published ones.^[8] The structure of this article is as follows. The analytical calculations are presented in Section 2. In Section 3, the tight-binding Hamiltonian is introduced. The results are explained and discussed in Section 4. In Section 5, the summary is presented.

2. Analytical calculations

2.1. Without applying strain

Many tight-binding Hamiltonian models have been proposed for monolayer MoS₂.^[20,24–27] Since, the $4d_{z^2}$ orbital is the dominant component near K and K' points, a single band general Hamiltonian in the basis of $(c_{\mathbf{k}\uparrow}, c_{\mathbf{k}\downarrow})$ can be written as^[8,29]

$$H_0(\mathbf{k} + \varepsilon \mathbf{K}) = \left(\frac{|\mathbf{k}|^2}{2m} - \mu \right) \sigma_0 + \alpha_R \mathbf{g}(\mathbf{k}) \cdot \boldsymbol{\sigma} + \varepsilon \beta_{so} \sigma_z, \quad (1)$$

where c_s is the electron annihilation operator, $s = \uparrow / \downarrow$ denotes the spin, $\varepsilon = \pm 1$ is the valley index, m is the effective mass of the electrons, and μ is the chemical potential measured from the conduction band minimum when SOC is omitted. $\mathbf{g}(\mathbf{k}) = (k_y, -k_x, 0)$ and α_R are the Rashba vector and RSOC strength coefficient, respectively. Finally, β_{so} is the ISOC strength coefficient and $\boldsymbol{\sigma}$ denotes the Pauli matrices. And σ_0 is the unit matrix.

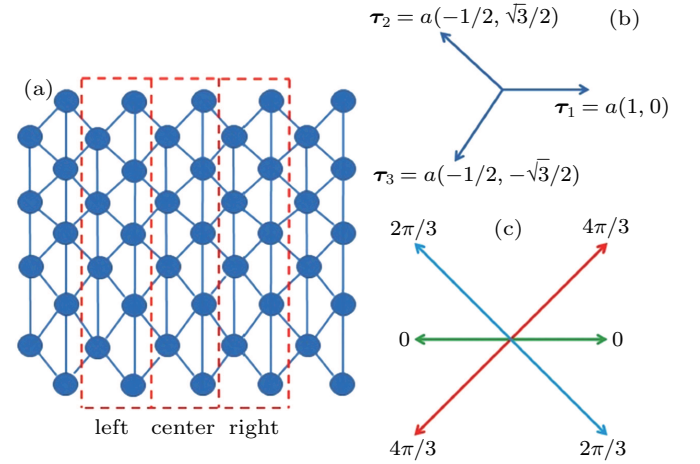


Fig. 1. (a) Triangular sublattice of monolayer Mo-atoms, (b) the bonding vectors of Mo-atoms, and (c) the nearest-neighbor pairing phases β_{ij} of the spin-singlet, p-wavelike phase.^[8]

The nearest-neighbor spin-singlet superconducting pairing amplitudes are proportional to $e^{-\beta_{ij}} \langle c_{i,\downarrow} c_{j,\uparrow} - c_{i,\uparrow} c_{j,\downarrow} \rangle$ in the two-dimensional representation.^[8] Here, β_{ij} is the nearest-neighbor pairing of the spin-singlet p-wavelike phase (see Fig. 1(c)).^[8] One can substitute the Fourier transformation of $c_{i,s}$ in the relation and show

$$\sum_{\langle ij \rangle} (c_{i,\downarrow} c_{j,\uparrow} - c_{i,\uparrow} c_{j,\downarrow}) = \sum_{\mathbf{k}} 2 \cos(\mathbf{k} \cdot \boldsymbol{\tau}_i) c_{-\mathbf{k},\downarrow} c_{\mathbf{k},\uparrow}, \quad (2)$$

where $\boldsymbol{\tau}_i$ are the bonding vectors of Mo-atoms, i.e., $\boldsymbol{\tau}_1 = a(1, 0)$, $\boldsymbol{\tau}_2 = a(-1/2, \sqrt{3}/2)$, $\boldsymbol{\tau}_3 = a(-1/2, -\sqrt{3}/2)$ with lattice constant $a = 3.16 \text{ \AA}$ (Fig. 1(b)), and $\mathbf{k} = k_x + ik_y$.^[8] Therefore,^[8]

$$\Delta(\mathbf{k}) = 2 \cos(ak_x) + e^{\frac{i2\pi}{3}} \left[\cos\left(-\frac{ak_x}{2}\right) + \cos\left(\frac{a\sqrt{3}}{2}k_y\right) \right] + e^{\frac{i4\pi}{3}} \left[\cos\left(-\frac{ak_x}{2}\right) + \cos\left(\frac{-a\sqrt{3}}{2}k_y\right) \right]. \quad (3)$$

By using Eqs. (1) and (3), in the basis of $(c_{k,\uparrow}, c_{k,\downarrow}, c_{-k,\uparrow}^\dagger, c_{-k,\downarrow}^\dagger)$, the general Bogoliubov–de Gennes (BdG) Hamiltonian can be written as^[8]

$$H_{\text{BdG}} = \begin{pmatrix} \varepsilon_k + \varepsilon\beta_{\text{so}} & i\alpha_{\text{R}}(k_x - ik_y) & 0 & \Delta(k) \\ -i\alpha_{\text{R}}(k_x + ik_y) & \varepsilon_k - \varepsilon\beta_{\text{so}} & -\Delta(k) & 0 \\ 0 & -\Delta^*(k) & -(\varepsilon_k + \varepsilon\beta_{\text{so}}) & -i\alpha_{\text{R}}(k_x + ik_y) \\ \Delta^*(k) & 0 & i\alpha_{\text{R}}(k_x - ik_y) & -(\varepsilon_k - \varepsilon\beta_{\text{so}}) \end{pmatrix}, \quad (4)$$

where $\varepsilon_k = \frac{k^2}{2m} - \mu$. It should be noted that $(c_{k,\uparrow}, c_{k,\downarrow})$ and $(c_{-k,\uparrow}^\dagger, c_{-k,\downarrow}^\dagger)$ are the basis vectors of electrons and holes, respectively. One can easily show that the eigenvalues of H_{BdG} are

$$E^2 = (\varepsilon_k^2 + \beta_{\text{so}}^2 + \alpha_{\text{R}}^2 k^2 + \Delta^2) \pm 2 [(\beta_{\text{so}}^2 + \alpha_{\text{R}}^2 k^2) \varepsilon_k^2 + \Delta^2 \beta_{\text{so}}^2]^{1/2}. \quad (5)$$

Using the Taylor expansion of Eq. (3) near the K (K') point, we have

$$\Delta(\mathbf{k} + \varepsilon\mathbf{K}) \approx \gamma\varepsilon(k_x + ik_y), \quad (6)$$

where $\gamma = 4\sqrt{3}$.^[8] The points Γ , K , and K' are rotation fixed points of threefold rotation.^[21] Therefore, we can study the change of the Chern number by the change of the rotation eigenvalues at the K and K' points (k_x & $k_y \rightarrow 0$).^[28] The eigenvalues of Eq. (4) at K -point are $E_1 = -\beta_{\text{so}} + \mu$, $E_2 = -\beta_{\text{so}} - \mu$, $E_3 = -\beta_{\text{so}} + \mu$, and $E_4 = \beta_{\text{so}} + \mu$ with eigenfunctions $\psi_1 = (1, 0, 0, 0)^T$, $\psi_2 = (0, 1, 0, 0)^T$, $\psi_3 = (0, 0, 1, 0)^T$, and $\psi_4 = (0, 0, 0, 1)^T$, respectively. Similarly, for K' -point we have $E'_1 = -\beta_{\text{so}} - \mu$, $E'_2 = -\beta_{\text{so}} + \mu$, $E'_3 = \beta_{\text{so}} + \mu$, and $E'_4 = -\beta_{\text{so}} + \mu$ with eigenfunctions $\psi'_1 = (1, 0, 0, 0)^T$, $\psi'_2 = (0, 1, 0, 0)^T$, $\psi'_3 = (0, 0, 1, 0)^T$, and $\psi'_4 = (0, 0, 0, 1)^T$, respectively. It should be noted that ψ_1 and ψ'_1 (ψ_2 and ψ'_2) are the eigenfunctions of the spin-up (down) electrons, but ψ_3 and ψ'_3

(ψ_4 and ψ'_4) are the eigenfunctions of the spin-up (down) holes in the basis of $(c_{k,\uparrow}, c_{k,\downarrow}, c_{-k,\uparrow}^\dagger, c_{-k,\downarrow}^\dagger)$.

2.2. With applying strain

It has been shown that the low-energy d-bands effective Hamiltonian around K -point and in the space of $(d_{z^2, \mathbf{k}, s}^e, d_{\varepsilon 2, \mathbf{k}, s}^e)$ can be written as^[15]

$$H_{k, \text{eff}}^{E, \varepsilon} = \begin{pmatrix} \Delta_c + \beta |\mathbf{k}|^2 & v\mathbf{k} + \kappa\mathbf{k}^{+2} \\ v\mathbf{k}^+ + \kappa\mathbf{k}^2 & \Delta_v + \alpha |\mathbf{k}|^2 + 2\varepsilon\beta_{\text{so}}s_z \end{pmatrix}, \quad (7)$$

where for MoS_2 , $\Delta_c = 1.78$ eV (conduction band edge), $\Delta_v = -0.19$ eV (valence band edge), $v = 2.44$ eV (group velocity), $\beta = 0.21$ eV·Å² (effective mass), $\alpha = 0.71$ eV·Å² (effective mass), $\kappa = 0.32$ eV·Å² (higher order in momentum trigonal corrections), $\beta_{\text{so}} = 0.06$ eV, and $s_z = \pm 1$.^[15] Of course, the cubic correction terms are omitted here.

The strain tensor of a two-dimensional membrane is given by^[13–15]

$$\varepsilon_{ij} = \frac{1}{2} \partial_i u_j + \partial_j u_i + (\partial_i h)(\partial_j h), \quad (8)$$

where $u(\mathbf{r})$ and $h(\mathbf{r})$ are in-plane and out-of-plane deformation vectors, respectively such that a generic atom at position \mathbf{r} is shifted to $\mathbf{r}' = \mathbf{r} + \mathbf{u}(\mathbf{r}) + \hat{z}h(\mathbf{r})$ under the deformation. Without curvature, equation (7) can be written as^[15]

$$H_{k, \text{eff}}^{E, \varepsilon} = \begin{pmatrix} \Delta_c + \beta |\mathbf{k} + \eta_2 F^\varepsilon|^2 + \delta_1 D + \delta_3 D^2 + s_z D(\delta\beta_{\text{so}1}) & v\mathbf{k} + \eta_1 F^\varepsilon + \kappa(\mathbf{k}^+ + \eta_4 F^{\varepsilon+})^2 \\ v\mathbf{k}^+ + \eta_1 F^{\varepsilon+} + \kappa(\mathbf{k} + \eta_4 F^\varepsilon)^2 & \Delta_v + \alpha |\mathbf{k} + \eta_3 F^\varepsilon|^2 + \delta_2 D + \delta_4 D^2 + s_z D(\delta\beta_{\text{so}2}) \end{pmatrix}, \quad (9)$$

where, $D = \text{Tr}[\varepsilon_{ij}]$ and $F^\varepsilon = (\varepsilon_{yy} - \varepsilon_{xx} + i\varepsilon_{xy})$.^[15] The values of all constants in Eq. (9) are provided in Ref. [15] and we do not repeat them here. From Eq. (9), it can be concluded that the terms $\beta |\eta_2 F^\varepsilon|^2 + \delta_1 D + \delta_3 D^2 + s_z D(\delta\beta_{\text{so}1})$ and $\alpha |\eta_3 F^\varepsilon|^2 + \delta_2 D + \delta_4 D^2 + s_z D(\delta\beta_{\text{so}2})$ should be added to Eq. (4) when we want to study the effect of strain on the topological properties at K and K' points (k_x & $k_y \rightarrow 0$). We will show that the off-diagonal terms are very small and in consequence they are negligible. It should be noted that it is assumed the crystal is flat and there is no any curvature under the applied deformations.

3. Tight-binding Hamiltonian

As it has been shown, the $4d_{z^2}$ orbital is the dominant component of the states near the CBM and the VBM located at K and K' points.^[2,8,12] Therefore, we consider a zigzag nanoribbon of Mo-layer with triangular crystal structure (Fig. 1(a)) and use a simple tight-binding Hamiltonian for studying the topological superconductivity in MoS_2 . Rostami *et al.* have shown that if the basis $\Psi_{\text{Mo}} = (d_{z^2}, d_{x^2-y^2}, d_{xy})$ is used, the Hamiltonian of Mo–Mo hopping can be written in k -space as^[31]

$$H_{\text{MM}} = \begin{pmatrix} \varepsilon_0 & 0 & 0 \\ 0 & \varepsilon_2 & -i\beta_{\text{so}, \text{Mo}} s_z \\ 0 & i\beta_{\text{so}, \text{Mo}} s_z & \varepsilon_2 \end{pmatrix}$$

$$+ 2 \sum_{i=1}^3 t_i^{\text{MM}} \cos(\mathbf{k} \cdot \boldsymbol{\tau}_i), \quad (10)$$

where ε_0 and ε_2 are the on-site energies, and t_i^{MM} is the hopping matrix in $\boldsymbol{\tau}_i$ direction (Fig. 1(b)). All constant values in Eq. (10) are provided in Ref. [29] and we do not repeat them here. In our real-space model, $\varepsilon_0 = 1.282$ eV, $\varepsilon_2 = 0.864$ eV, and hopping terms $t_i = 2t_i^{\text{MM}}$ are assumed. It should be noted that the Mo-S and S-S hopping terms are not considered, and in consequence, the values are assumed such that the next results not only provide the correct physics but also confirm the results of analytical calculations. Figure 1 shows a zigzag nanoribbon of Mo-atoms in triangular lattice structure. Using Eq. (10) in real-space,^[29] one can consider the central, left, and right supercells and write their Hamiltonian matrices H_{00} , H_{01} , and H_{01} respectively. The energy dispersion curve of the nanoribbon can be found by finding the eigenvalues of the following Hamiltonian:

$$H^{\uparrow(\downarrow)} = H_{00}^{\uparrow(\downarrow)} + e^{i\mathbf{k} \cdot \mathbf{A}} H_{01}^{\uparrow(\downarrow)} + e^{-i\mathbf{k} \cdot \mathbf{A}} H_{10}^{\uparrow(\downarrow)}, \quad (11)$$

where \mathbf{A} is the lattice vector of the nanoribbon. Since, $s_z = +1$ (-1) for spin-up (\uparrow) (down (\downarrow)) electrons, we can write the Hamiltonians for both types of spins. In each supercell, the nearest-neighbor pairing term is equal to $\Delta_0 e^{i\beta_{ij}}$ in real-space where β_{ij} depends on the direction ($\boldsymbol{\tau}_i$) as shown in Fig. 1(c).^[8] It is assumed that the pairing happens only between the $4d_{z^2}$ orbitals.^[30] Therefore, the pairing matrix between two Mo-nearest neighbor atoms can be written as

$$\Delta = \Delta_0 e^{i\beta_{ij}} \begin{pmatrix} 1 & 0 & 0 \\ 0 & 0 & 0 \\ 0 & 0 & 0 \end{pmatrix}. \quad (12)$$

However, the Hamiltonian of holes is equal to $-H^{*e}(-\mathbf{k})$, where $H^e(\mathbf{k})$ is the Hamiltonian of electrons.^[8] Thus, one can write the BdG-Hamiltonian as

$$H_{\text{BdG}} = \begin{pmatrix} H^{e,\uparrow} & R & 0 & \Delta \\ R^+ & H^{e,\downarrow} & -\Delta & 0 \\ 0 & -\Delta^* & H^{h,\uparrow} & R^+ \\ \Delta^* & 0 & R & H^{h,\downarrow} \end{pmatrix}, \quad (13)$$

where R stands for RSOC which is assumed to be equal to zero in the next calculations because we study the superconductivity effect at K (K')-point. It should be noted that for adding the RSOC effect to the model, one should find its analytical formula in the basis $\psi_{\text{Mo}} = (d_{z^2}, d_{x^2-y^2}, d_{xy})$.

Another simple model can be used to study the effect of the chemical potential, respect to the ISOC strength, on the topological properties of MoS₂. In this model, only the d_{z^2} orbital is considered, and the term $-\mu + \varepsilon\beta_{\text{so}}$ is placed on the diagonal of $H_{00}^{\uparrow(\downarrow)}$. For hopping between two Mo-nearest neighbor atoms, the hopping energy $t = (3V_{\text{dd}\delta} + V_{\text{dd}\sigma})/2$ is used in all directions^[29] and the above explained method is followed again. It should be noted that in calculations, $\Delta = \Delta_0 e^{i\beta_{ij}}$,^[8] $V_{\text{dd}\delta} = 0.228$ eV, and $V_{\text{dd}\sigma} = -0.895$ eV.^[29]

4. Results and discussion

The eigenvalues of Eq. (4) at K and K' points were found in Section 2. Figure 2 shows them schematically. As Fig. 2 shows, the curves of negative energies touch the curves of positive energies at two points A and B which are called the band-inversion (nodal) points. However, the points are placed on the line $E/\beta_{\text{so}} = 0$. Therefore, band closing happens at K and K' points. Since the K and K' points are rotation fixed points, it is possible to label the states at the fixed points by their rotation eigenvalues which are $e^{i\pi(2p-1)/n}$ with $p = 1, 2, \dots, n$ (fold).^[22] If R stands for the rotation matrix for both electron and hole, a BdG Hamiltonian is rotation-invariant if it satisfies^[28]

$$\overline{R}V H_{\text{BdG}}(\mathbf{k}) \overline{V}^+ \overline{R}^+ = H_{\text{BdG}}(R\mathbf{k}), \quad (14)$$

where $\overline{R} = \text{diag}(R, R^*)$, $\overline{V} = \text{diag}(1, e^{-i\varphi})$, and $\varphi = 2\pi/3$. The elements $(R, 1)$ and $(R^*, e^{-i\varphi})$ act on the electron and hole, respectively.^[28] Also, $R = \exp(i\sigma_z \pi/3)$ for σ_z on spin,^[30] and

$$R \begin{pmatrix} c_{k,\uparrow}^{e,+} \\ c_{k,\downarrow}^{e,+} \end{pmatrix} = \begin{pmatrix} e^{i\pi/3} & 0 \\ 0 & e^{-i\pi/3} \end{pmatrix} \begin{pmatrix} c_{k,\uparrow}^{e,+} \\ c_{k,\downarrow}^{e,+} \end{pmatrix} \\ = \begin{pmatrix} e^{i\pi/3} c_{k,\uparrow}^{e,+} \\ e^{-i\pi/3} c_{k,\downarrow}^{e,+} \end{pmatrix}. \quad (15)$$

That is $\begin{pmatrix} c_{k,\uparrow}^{e,+} \\ c_{k,\downarrow}^{e,+} \end{pmatrix} \rightarrow \begin{pmatrix} e^{i\pi/3} c_{k,\uparrow}^{e,+} \\ e^{-i\pi/3} c_{k,\downarrow}^{e,+} \end{pmatrix}$ for electrons, and for

holes $\begin{pmatrix} c_{-k,\downarrow}^e \\ c_{-k,\uparrow}^e \end{pmatrix} \rightarrow \begin{pmatrix} e^{i(\frac{\pi}{3}-\varphi)} c_{-k,\downarrow}^e \\ e^{-i(\frac{\pi}{3}-\varphi)} c_{-k,\uparrow}^e \end{pmatrix} = \begin{pmatrix} e^{-i\pi/3} c_{-k,\downarrow}^e \\ e^{-i\pi} c_{-k,\uparrow}^e \end{pmatrix}$.^[28]

By considering the diagonal Hamiltonian $\text{diag}(E_1, E_2, E_3, E_4)$ at K -point, if $|\mu| > |\beta_{\text{so}}|$ then the eigenvalues E_1 and E_2 (E'_1 and E'_2) are negative, and the eigenvalues E_3 and E_4 (E'_3 and E'_4) are positive. But, if $|\mu| < |\beta_{\text{so}}|$ then the eigenvalues E_2 and E_3 (E'_1 and E'_4) are negative, and the eigenvalues E_1 and E_4 (E'_2 , and E'_3) are positive. Therefore, for $|\mu| > |\beta_{\text{so}}|$ the rotation eigenvalues (η_i , $i = 1, 2, 3, 4$) are $e^{-i\pi/3}$, $e^{-i\pi}$, $e^{i\pi/3}$, and $e^{-i\pi/3}$ which are related to E_1 , E_2 , E_3 , and E_4 , respectively at K -point. It means that $\overline{R}\overline{V} = \text{diag}(e^{-i\pi/3}, e^{-i\pi}, e^{i\pi/3}, e^{-i\pi/3})$.^[28] Also, for $|\mu| < |\beta_{\text{so}}|$, they are $e^{i\pi/3}$, $e^{-i\pi}$, $e^{-i\pi/3}$, and $e^{-i\pi/3}$ at K -point, and in consequence, $\overline{R}\overline{V} = \text{diag}(e^{i\pi/3}, e^{-i\pi}, e^{-i\pi/3}, e^{-i\pi/3})$.^[28] Similarly, it can be shown that at K' -point, for $|\mu| > |\beta_{\text{so}}|$, $\overline{R}\overline{V}^+ = \text{diag}(e^{-i\pi/3}, e^{-i\pi}, e^{i\pi/3}, e^{-i\pi/3})$ and for $|\mu| < |\beta_{\text{so}}|$, $\overline{R}\overline{V}^+ = \text{diag}(e^{i\pi/3}, e^{-i\pi}, e^{i\pi/3}, e^{-i\pi/3})$.^[28] if the diagonal Hamiltonian is written as $\text{diag}(E'_1, E'_2, E'_3, E'_4)$. But, the Chern number (C) in the three-fold symmetric system can be written as^[22,28]

$$e^{-i2\pi C/3} = \prod_{i \in \text{occ.}} \eta_i(K) \eta_i(K'). \quad (16)$$

As a result, for $|\mu| > |\beta_{\text{so}}|$,

$$E_1 = E'_2 = -\mu + \beta_{\text{so}} < 0 \rightarrow$$

$$e^{-i2\pi C/3} = e^{-i\pi/3} e^{-i\pi} = e^{-i4\pi/3} \rightarrow C = 2, \quad (17)$$

$$E_2 = E'_1 = -\mu - \beta_{so} < 0 \rightarrow$$

$$e^{-i2\pi C/3} = e^{-i\pi} e^{-i\pi/3} = e^{-i4\pi/3} \rightarrow C = 2. \quad (18)$$

Similarly, for $|\mu| < |\beta_{so}|$,

$$E_2 = E'_1 = -\mu - \beta_{so} < 0 \rightarrow$$

$$e^{-i2\pi C/3} = e^{-i\pi} e^{+i\pi/3} = e^{-i2\pi/3} \rightarrow C = 1, \quad (19)$$

$$E_3 = E'_4 = \mu - \beta_{so} < 0 \rightarrow$$

$$e^{-i2\pi C/3} = e^{-i\pi/3} e^{-i\pi/3} = e^{-i2\pi/3} \rightarrow C = 1. \quad (20)$$

However, for two-dimensional materials, it has been shown that^[3]

$$C_{2D} = \sum_{n \in \text{occ.}} C^{(n)}. \quad (21)$$

Therefore, for $|\mu| > |\beta_{so}|$, $C_{2D} = 4$, for $|\mu| < |\beta_{so}|$, $C_{2D} = 2$, otherwise it is equal to zero.^[8] The topological classification of superconductors described by the BdG equation can be found in the periodic table of Altland–Zirnbauer.^[32] When the time reversal symmetry is absent, the BdG-superconductors are classified into two classes called C and D. In C (D)-class, the sublattice symmetry (SLS) is absent and the particle–hole symmetry (PHS) is -1 ($+1$).^[32,33] It has been shown that in monolayer MoS₂, the time reversal symmetry is spontaneously broken in the E irreducible representation of C_{3v} and the pairing matrix has spin-singlet p-wave characteristic.^[8] Therefore, PHS is -1 and $SU(2)$ spin-1/2 rotation is preserved. It means that the topological superconductor belongs to C-class.

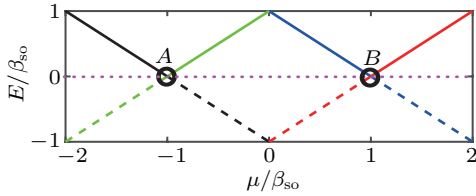


Fig. 2. Energy dispersion curve (phase diagram) of superconducting MoS₂ at K (K')-point. The dashed and filled lines show the negative and positive energies, respectively. The points A and B stand for band-inversion (nodal) points. The general equation $E/\beta_{so} = \pm(1 \pm \mu/\beta_{so})$ is used here.

Let us consider a nanoribbon of Mo-atoms with zigzag edge as shown in Fig. 1(a) and use Eqs. (10) (in real-space) and (11) to find the energy dispersion curve $E(k)$. It can be shown that the edge states can also be found for the flat edge of the triangular lattice of Mo layer.^[8] Therefore, the similar behavior is expected. Figure 3(a) shows the energy dispersion curve of the nanoribbon. As it shows, the valence and conduction bands intersect with each other and since the DOS at zero energy has significant value (Fig. 3(b)), there are surface states and the ribbon behaves as a metal. It should be noted that the RSOC is not considered here. Since we assume $\beta_{so} = 60$ meV,^[29] the difference between spin up and down electrons is negligible, and it is not shown.

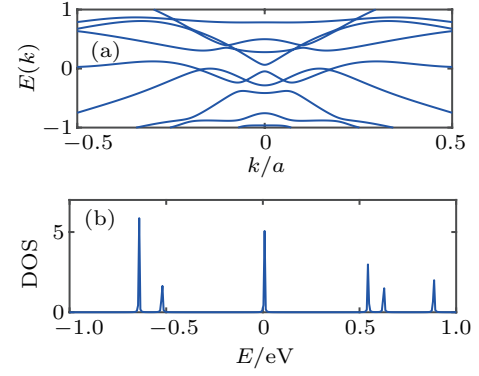


Fig. 3. (a) Energy dispersion curve of a zigzag nanoribbon of Mo atoms and (b) density of states.

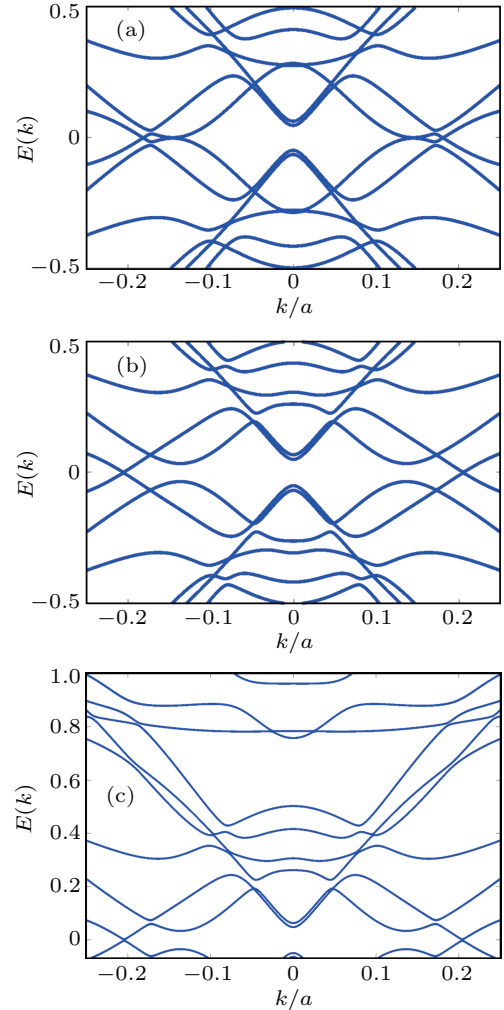


Fig. 4. Energy dispersion curve of BdG Hamiltonian with (a) $\beta_{so} = 60$ meV, $\Delta_0 = 6$ meV, (b) $\beta_{so} = 6$ meV, $\Delta_0 = 60$ meV, and (c) $\beta_{so} = 60$ meV, $\Delta_0 = 60$ meV. The RSOC = 0 here. Each supercell includes 9 Mo atoms.

By using the model of zigzag nanoribbon described in Eqs. (12) and (13), the energy dispersion curve of the BdG Hamiltonian is found without RSOC. Figures 4(a) and 4(b) show the $E(k)$ curves for $\beta_{so} > \Delta_0$ and $\beta_{so} < \Delta_0$. As Fig. 4(a) shows, there are four zero energy states when $\beta_{so} > \Delta_0$ while it decreases to two for $\beta_{so} < \Delta_0$. In addition, figure 4(c) shows that there are zero energy states when $\beta_{so} = \Delta_0$. Therefore, it can be concluded that the model can predict the same topological properties which were found by using the Eqs. (16)–(21)

above. The zero energy states are referred to the Majorana states.

Here, the simpler model which was introduced at the end paragraph of Section 3 is used to study the effect of chemical energy in respect to the ISOC strength. Figure 5(a) shows the energy dispersion curve when $\beta_{so} = 60$ meV, $\Delta_0 = 6$ meV, and $\mu = 87$ meV.^[30] As it shows, since $\mu > \beta_{so}$, there are four zero energy states while for $\mu = 57$ meV, there are two zero energy states (Fig. 5(b)). The model shows that when $\mu \gg \beta_{so}$, a gap is opened in the curve (it is not shown in the figures). Finally, as Fig. 6 shows, the DOS has significant values at zero energy for both cases, i.e., $\mu > \beta_{so}$ and $\mu < \beta_{so}$. Therefore, the simple model can explain the analytical results qualitatively (at least). Through fourth-order Ginzburg–Landau analysis, Yuan *et al.* have shown that the time reversal symmetry is spontaneously broken in the E irreducible representation of C_{3v} and this phase is characterized by Chern numbers and supports Majorana edge states.^[8] In Fig. 4, the edge states can be recognized for $E = 0$ eV which are related to the different Chern numbers. These edge states are attributed to the Majorana state.^[8]

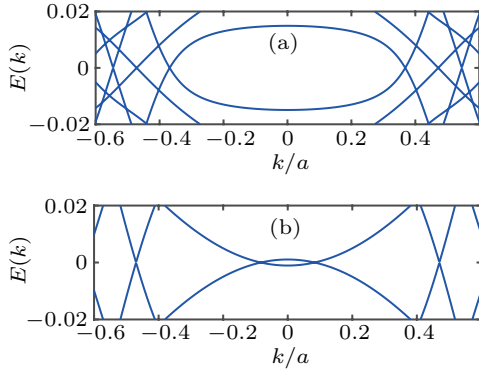


Fig. 5. Energy dispersion curve of BdG Hamiltonian with (a) $\mu = 87$ meV and (b) $\mu = 57$ meV. Here, $\beta_{so} = 60$ meV, $\Delta_0 = 6$ meV, and RSOC strength is equal to zero. Each supercell includes 9 Mo atoms.

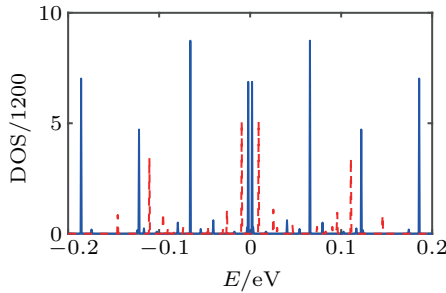


Fig. 6. Density of states versus energy for $\mu > \beta_{so}$ in filled blue color and for $\mu < \beta_{so}$ in dashed red color. Here, RSOC strength is equal to zero. Each supercell includes 9 Mo atoms.

It should be noted that, the intrinsic unconventional superconductivity has been observed in twisted bilayer Graphene.^[34] Po *et al.* have invoked SU(4) ferromagnetism interaction^[35] and Xu *et al.* have invoked an effective anti-ferromagnetic interaction^[36] for explaining the effect, while both have considered an effective triangular superlattice.^[34,35]

We considered a triangular lattice too. But, for doing the numerical calculations we considered the $(d_{z^2}, d_{x^2-y^2}, d_{xy})$ orbitals and assumed that the pairing happens only between the $4d_{z^2}$ orbitals while Xu *et al.* have considered a two-orbital Hubbard model.^[36] Also, we considered the spin-singlet p-wavelike phase while they have expected the d-wave pairing to be favored.

Finally, the effect of mechanical transformation on the topological properties of monolayer MoS₂ is investigated. An uniaxial tension field (T) is applied to the Mo-plane. The vector T has the angle θ with the x -axis which is in parallel with the zigzag edge of the nanoribbon. It can be shown that the strain tensor (ε) can be written as^[33]

$$\varepsilon = \tau \begin{pmatrix} \cos^2 \theta - v_{\parallel} \sin^2 \theta & (1 + v_{\parallel}) \sin \theta \cos \theta & 0 \\ (1 + v_{\parallel}) \sin \theta \cos \theta & \sin^2 \theta - v_{\parallel} \cos^2 \theta & 0 \\ 0 & 0 & -v_{\perp} \end{pmatrix}, \quad (22)$$

where τ is the tension strain, and v_{\parallel} and v_{\perp} are the in-plane and out-of-plane Poisson's ratios, respectively. Therefore,

$$D = \text{Tr}[\varepsilon_{ij}] = \tau(1 - v_{\parallel} - v_{\perp}), \quad (23)$$

and for $\theta = 0$, i.e., T is parallel to the zigzag edge,

$$F^E = (\varepsilon_{yy} - \varepsilon_{xx} + i\varepsilon_2\varepsilon_{xy}) = \tau(-1 + v_{\parallel}), \quad (24)$$

for $\theta = \pi/2$, i.e., T is perpendicular to the zigzag edge,

$$F^E = (\varepsilon_{yy} - \varepsilon_{xx} + i\varepsilon_2\varepsilon_{xy}) = \tau(1 - v_{\parallel}). \quad (25)$$

By using the values of all constants at Eq. (9) which were provided before,^[13–15] it can be shown that

$$\begin{aligned} & \beta |\eta_2 F^E|^2 + \delta_1 D + \delta_3 D^2 + s_z D (\delta \beta_{so1}) \\ & = -0.0844 + 0.07s_z, \end{aligned} \quad (26)$$

$$\begin{aligned} & \alpha |\eta_3 F^E|^2 + \delta_2 D + \delta_4 D^2 + s_z D (\delta \beta_{so2}) \\ & = -0.4295 - 0.0142s_z, \end{aligned} \quad (27)$$

$$\eta_1 F^E + \kappa \eta_4^4 F^{E2} = -7.58 \times 10^{-4}, \quad (28)$$

which is negligible. These values should be added to Eqs. (17)–(20). However, as we assumed that the tension field does not change the rotation symmetry (i.e., it is small), these equations are satisfied, and in consequence, the topological properties are preserved under the small uniaxial tensions field.

It should be noted that one can calculate the effect of biaxial strain similarly. For example, under trigonal deformation such as $(u_x, u_y) = \frac{u_0}{2} (xy, \frac{x^2-y^2}{2})$, by using Eq. (8), one can easily show that $F^E = u_0(y-x)$. Also, for arc-shape deformation $(u_x, u_y) = (\frac{xy}{R}, \frac{-x^2}{2R})$, where R is the arc radius, $F^E = (\frac{y}{R}, 0)$. But, the deformed new Hamiltonian is now given by Eq. (50) of Ref. [15] and the effect of curvature and gauge fields should be considered. Finally, the effect of deformation on the topological properties can be studied by calculating the amount of

each element of the new Hamiltonian, if the deformation does not change the symmetry of the lattice.

As the electronic properties of two-dimensional materials are studied near K and K' points in this research, the behavior of energy dispersion curve near these points is considered. But, for studying the effect of other orbitals, complete Hamiltonian, i.e., Eq. (2) of Ref. [31], should be considered. Then, equations (34)–(37) of Ref. [15] can be used to calculate the effect of deformation. Obviously, the calculation method is more complicated than the provided method in this article and needs more justification. The effect of doping can be only studied by using the *ab-initio* methods such as density functional theory, which is out of the scope of this article.

5. Summary

It has been shown that the $4d_{z^2}$ orbital is the dominant component of the states near the CBM and the VBM located at K and K' points in the monolayer MoS_2 . We have considered the triangular lattice of Mo-plane and studied the topological superconductivity in monolayer MoS_2 . By considering the spin-singlet pairing at K and K' points, we have shown that the BdG-Hamiltonian matrix is diagonal and has four distinct eigenvalues which are functions of chemical energy and ISOC strength. By using the rotation symmetry of the fixed points K and K' , it has been shown that the Chern number is equal to four (two) when the chemical potential μ is greater (smaller) than ISOC strength β_{so} and otherwise it is equal to zero. Also, we have introduced two simple tight-binding BdG-Hamiltonian models for finding the zero energy states (i.e., Majorana states) and confirming the analytical results. In the first model, the ISOC was considered by choosing the $d_{x^2-y^2}$ and d_{xy} orbitals of Mo-atoms. We have shown that when β_{so} is greater than pairing potential Δ_0 , there are four zero energy states. Under the same condition and using the second single-band tight-binding Hamiltonian, we have shown that for both $\mu > \beta_{\text{so}}$ and $\mu < \beta_{\text{so}}$, there are zero energy states and for $\mu \gg \beta_{\text{so}}$, a gap is opened in the energy dispersion curve. Finally, we have shown that under small uniaxial strain which can be parallel or perpendicular to the zigzag edge of Mo-nanoribbon, the topological properties are preserved.

References

[1] Kaasbjerg K, Thygesen K S and Jacobsen K W 2012 *Phys. Rev. B* **85** 115317

- [2] Roldan R, Cappelluti E and Guinea F 2013 *Phys. Rev. B* **88** 054515
- [3] Ye J T, Zhang Y J, Akashi R, Bahramy M S, Arita R and Iwasa Y 2012 *Science* **338** 1193
- [4] Taniguchi K, Matsumoto A, Shimotani H and Takagi H 2012 *Appl. Phys. Lett.* **101** 042603
- [5] Ochoa H and Roldan R 2013 *Phys. Rev. B* **87** 245421
- [6] Klinovaja J and Loss D 2013 *Phys. Rev. B* **88** 075404
- [7] Kormanyos A, Zolyomi V, Drummond N D and Burkard G 2014 *Phys. Rev. X* **4** 011034
- [8] Yuan N Q, Mak K F and Law K T 2014 *Phys. Rev. Lett.* **113** 097001
- [9] Lu J M, Zeliuk O, Leemakers I, Yuan N D Q, Zeitler U, Law K T and Ye J T 2015 *Science* **350** 1353
- [10] Khezerlou M and Goudarzi H 2016 *Phys. Rev. B* **93** 115406
- [11] Bardeen J, Cooper L N and Schrieffer J R 1957 *Phys. Rev.* **108** 1175
- [12] Zeng S, Zhao Y, Li G and Ni J 2016 *Phys. Rev. B* **94** 024501
- [13] Jiang J W, Qi Z, Park H S and Rabczuk T 2013 *Nanotechnology* **24** 435705
- [14] Woo S, Park H C and Son Y W 2016 *Phys. Rev. B* **93** 075420
- [15] Pearce A J, Mariani E and Burkard G 2016 *Phys. Rev. B* **94** 155416
- [16] Zhang J J, Gao B and Dong S 2016 *Phys. Rev. B* **93** 155430
- [17] Szczesniak R, Durajski A P and Jarosik M W 2018 *Front. Phys.* **13** 137401
- [18] Kang M, Jung S W, Shin W J, Sohn Y, Ryn S H, Kim T K, Hoesch M and Kim S 2018 *Nat. Mater.* **17** 676
- [19] He W Y, B Zhou T, He J J, Yuan N F Q, Zhang T and Law K T 1999 *Nat. Phys.* **1** 40
- [20] Xiao D, Liu G B, Feng W, Xu X and Yao W 2012 *Phys. Rev. Lett.* **108** 196802
- [21] Cappelluti E, Roldan R, Silva-Guillen J A, Ordejon P and Guinea F 2013 *Phys. Rev.* **88** 075409
- [22] Benalcazar W A, Teo J C Y and Hughes T L 2014 *Phys. Rev. B* **89** 224503
- [23] Zahid F, Liu L, Zhu Y, Wang J and Guo H 2013 *AIP Advan.* **3** 052111
- [24] Liu G B, Shan W Y, Yao Y, Yao W and Xiao D 2013 *Phys. Rev. B* **88** 085433
- [25] Rostami H, Moghaddam A G and Asgari R 2013 *Phys. Rev. B* **88** 085440
- [26] Ridolfi E, Le D, Rahman T S, Mucciolo E R and Lewenkopf C H 2015 *J. Phys. Condens. Matter* **27** 365501
- [27] Rostami H, Asgari R and Guinea F 2016 *J. Phys. Condens. Matter* **28** 495001
- [28] Huang S M, Tsai W F, Chung C H and Mou C Y 2016 *Phys. Rev. B* **93** 054518
- [29] Rostami H, Roldan R, Cappelluti E, Asgari R and Guinea F 2015 *Phys. Rev. B* **92** 195402
- [30] Sato M and Ando Y 2017 *Rep. Prog. Phys.* **80** 076501
- [31] Farokhnezhad M, Esmailzadeh M and Shakouri Kh 2017 *Phys. Rev. B* **96** 205416
- [32] Chiu C K, Teo J C Y, Schnyder A P and Ryu S 2016 *Rev. Mod. Phys.* **88** 035005
- [33] Schnyder A P, Ryu S, Furusaki A and Ludwig A W W 2008 *Phys. Rev. B* **78** 195125
- [34] Cao Y, Fatemi V, Feng S, Watanabe K, Taniguchi T, Kaxiras E and Herrero P J 2018 *Nature* **556** 43
- [35] Po H C, Zou L, Vishwanath A and Senthil T 2018 *Phys. Rev. X* **8** 031089
- [36] Xu C and Balents L 2018 *Phys. Rev. Lett.* **121** 087001